THE JOURNAL OF PHYSICAL CHEMISTRY A
A JOURNAL OF THE AMERICAN CHEMICAL SOCIETY

pubs.acs.org/JPCA

Article

Computational Study on the Effect of Thienyl π-Donor on the Optical Response of Nonclassical Oligo-Pyrazinothienothiadiazole Biradicaloids

Anup Thomas, Mahesh G. Wakhradkar, Siddlingeshwar B,* Krishna Chaitanya Gunturu,* Anna Kaczmarek-Kędziera,* and Joel Abraham

Cite This: *J. Phys. Chem. A* 2022, 126, 7829−7839

Read Online

ACCESS | Metrics & More | Article Recommendations

ABSTRACT: Computational analyses were performed on nitrogen-rich oligothiadizolothiophenes $\mathbf{TT}_n$ (n = 0−3) and their four π-donor-substituted derivatives $\mathbf{Th\text{-}TT}_n$ (n = 0−3) to examine the optical response due to geometrical and electronic structural attributes in the longitudinal and transverse axes, respectively. Our results are understood in the context of greater conjugation in the longitudinal axis (via additional fused rings) and substitution of a thienyl π-donor in the transverse axis of the geometry of each derivative. On inspection of the frontier molecular orbitals, we found that the better electron-accepting ability with minimal sacrifice in the ionization potentials results from geometrical aspects in both longitudinal and transverse axes. Due to the narrowed highest occupied molecular orbital−lowest unoccupied molecular orbital gaps, all of the derivatives exhibit a biradicaloid character (BRC) and one-photon panchromatic absorption; however, the open-shell nature weakened the charge transfer characteristics of excitation. In both the series, the odd electron density distributions and electron localization plots amply demonstrate the weakening of ylide character in fused thiophene rings and clearly indicate to the emergence of a long-bond/single BRC in the sulfurdimithide moiety in both series. In addition, the estimated tensor components of the second hyperpolarizability as well as overall responses confirm the shift from the longitudinal to transverse axis following the substitution with the π-donor. Interestingly, the TPA cross sections show comparable behavior, but contrary to γ, π-donor thienyl substitution appears to be discouraging in getting higher TPA responses for higher homologous series. Therefore, this study opens a new conjecture on tuning better nonlinear optical properties of organic functional materials.

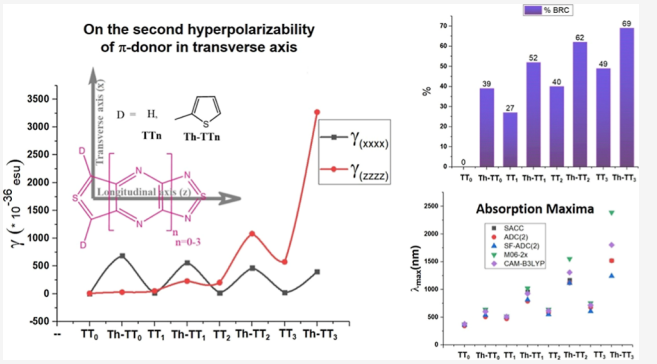

INTRODUCTION

The constantly growing requirements for high-speed data processing and optical communication regimes call for the need of materials having high nonlinear optical (NLO) activity, specifically the macroscopic third order susceptibility χ^3, which in turn is related to molecular second hyperpolarizability γ.[1−3] Of these materials, organic dyes are keenly explored due to their fast response, flexibility in molecular design, and film-forming ability, which allow a low-cost fabrication. These features have fuelled research and development in organic photonic materials both in academics and in the industry. The search for new and efficient photonic material remains one of the most active areas in this field.[4,5] While bringing out efficient devices is one challenge, understanding the molecular electronic structure by doing quantum mechanical computation to elucidate design principles to tune and thus enhance the hyperpolarizability is another.[6]

Two important molecular-level design parameters that are posited to be important to achieve large hyperpolarizabilities are minimizing the electronic excitation energy and/or maximizing the transition dipole moments as well as the difference in the dipole moment between ground and excited states.[7,8] Routinely small excitation energy is achieved by increasing the π-conjugation, and further lessening occurs when end-capped with donors (D) and/or acceptors (A).[9] The -D and -A substitutions introduce intramolecular charge transfer (ICT) characteristics and result in increased transition moments.[10] A successfully utilized concept to obtain large differences in dipole moment upon excitation is by twisting the π bonding region of the D−π−A system, owing to the

Received: July 7, 2022
Revised: October 7, 2022
Published: October 24, 2022

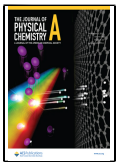

https://doi.org/10.1021/acs.jpca.2c04788
J. Phys. Chem. A 2022, 126, 7829−7839

formation of a charge separated zwitterionic-like ground-state. With these design schemes, many compounds having large NLO properties were synthesized.[5]

Along with that, Fabian and Zahradník have qualitatively proposed a less conventional alternative approach to achieve a small highest occupied molecular orbital (HOMO)−lowest unoccupied molecular orbital (LUMO) gap (HLG) (in line with that the excitation energy also decreases) by removing the orbital degeneracy of frontier non-bonding molecular orbitals of a biradical.[9] To get rid of the degeneracy, one has to do heteroatom substitutions and/or allow the spins to effectively delocalize via lengthening the conjugated π-framework and ultimately lead to stable biradicaloids.[11−13] Bhanuprakash and co-workers have shown that in many cases, excitation energy shrinks as the biradicaloid character (BRC) proliferates.[14,15] In the meantime, Nakano and colleagues found a very interesting and important relationship between BRC and NLO activity.[16] Their experimental and theoretical studies have confirmed that the magnitudes of second hyperpolarizability values are larger for the molecules having moderate BRC when compared with analogues closed-shell and extreme biradical systems.[17,18] It was also observed that the outspreading of conjugation by fused rings also increases the BRC as well as second hyperpolarizability.[19] In the light of the above correlation, several symmetric molecules such as diphenalenyl diradicaloids, quinoidal oligothiophenes, graphene nanoflakes, dicyclopenta-fused acenes, and molecules having a paraquinodimethine biradical substructure are designed and their large NLO responses were demonstrated experimentally and validated the theoretical predictions.[20] In addition to that, they also demonstrated that the NLO properties augment when the structure is asymmetric.[21]

As far as is known, all these NLO studies on biradicaloid systems are mainly focused on the second hyperpolarizability by expanding the π conjugation on the longitudinal axis by incorporating additional fused rings. In this study, we would like to computationally explore the effect of augmenting symmetric quadruple type ICT by a π donor substitution on the transverse axis along with the linear extension of fused planar π-rings in the longitudinal axis (Scheme 1). Thus, the

Scheme 1. Schematic Representation of Oligothiadizolothiophenes Considered in This Work

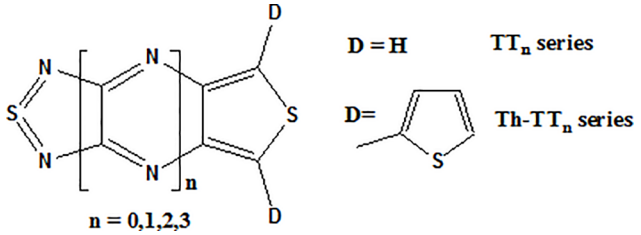

molecules chosen for this study are nonclassical nitrogen-rich oligothiadizolothiophenes $\mathbf{TT}_n$ (where n = 0−3) and the four π-D-substituted derivatives of each one. Our earlier valence bond and molecular orbital studies have revealed a BRC in the experimentally synthesized near infrared (NIR) absorbing donor-substituted thienothiadiazole ($\mathbf{TT}_0$) and thiadiazolothienopyrazine ($\mathbf{TT}_1$) derivatives, which are earlier believed to be closed-shell species.[11,15] On the contrary, the experiments later confirmed that a positional isomer of $\mathbf{TT}_1$ has a biradicaloid nature.[22,23] Hence, the validity of DFT predictions has been established through experimental studies in this class of molecules. The long-wavelength electronic absorption feature was speculatively credited to the presence of hypervalent bonding and termed as super acceptors.[24] This contradicts our earlier finding, and we have hypothesized that NIR absorption of these nonclassical dyes is the result of the interplay between charge transfer (CT) and BRC.[11,15] Similarly, $\mathbf{TT}_2$ and $\mathbf{TT}_3$ are the structures where the central pyrazine ring of $\mathbf{TT}_0$ is replaced with pyrazino[2,3-*b*]pyrazine and dipyrazino[2,3-*b*:2′,3′-*e*]pyrazine ring, respectively. It is included in this study even though $\mathbf{TT}_2$ and $\mathbf{TT}_3$ have not yet been synthesized. The fused ring extension is known to increase the singlet BRC and in parallel, with that, the excitation energy decreases. Donor substitution further amplifies the BRC.[25] The presence of a nitrogen heteroatom brings together stability, ring asymmetry (in longitudinal axis), and enhanced dipole moments in the structure. We hope that this study regarding these combined effects of substitution (ICT, BRC, and asymmetry) on NLO behavior such as second hyperpolarizability and two-photon absorption (TPA) characteristics will expand the understanding of design criteria to enhance NLO responses.

Computational Methodology. The geometries for simulating optoelectronic properties in this study are optimized using M06-2x hybrid meta GGA functional with 54% Hartree−Fock (HF) exchange and a cc-PVTZ basis set. Vibrational frequency analysis is then performed on computed geometries, confirming that optimized structures have no imaginary frequencies, that is, to ensure that the obtained geometries are minimum on the respective potential energy surfaces. The TDDFT/RPA method is used to evaluate the wavelength of the absorption maxima of the first two dipole-allowed electronic transitions. For the prediction of electronic absorption, the CAM-B3LYP and M06-2X functionals are used for comparison. To judge the adequacy of TDDFT for describing one-photon absorption, three post-HF methods have been used: symmetry-adapted cluster configuration interaction (SAC-CI), algebraic diagrammatic construction scheme in the second-order perturbation scheme [ADC(2)], and its spin-flip variant SF-ADC(2).[26−28] The split basis set 6-31G(d,p) and augmented correlation consistent basis set jun-cc-pVDZ(d,p) have been used in SAC-CI and ADC(2) calculations, respectively. The SAC-CI calculations are carried out at level one with an active space of 120 orbitals (40 occupied orbitals and 80 unoccupied orbitals) except for TT0 (the smallest system of the series) for which a full window is considered. In these molecules, the extent to which they possess an open shell is determined by the natural orbital occupancy number of the LUMO orbital of a broken-symmetry (BS) LC-UBLYP wave function. Odd electron density (OED) distribution and CT analysis have been performed by post-processing the wave functions obtained by BS-LCBLYP and CAM-B3LYP methods using the Multiwfn package.[29] The NLO parameters are determined at the BS-LCBLYP/6-311+G(d,p) level, and the TPA cross sections are determined using the CAM-B3LYP/6-31+G(d,p) method, which provides the reasonable cost-to-performance ratio and although underestimating significantly the TPA strength, allows us to obtain the correct relative tendencies for extended systems.[30−35] All DFT, TDDFT, and SAC-CI calculations were performed using G16 software, Dalton2021.alpha (2020) code is used for TPA cross section calculations, and Q-Chem.5.4 for ADC(2) and SF-ADC(2) calculations.[36−39]

https://doi.org/10.1021/acs.jpca.2c04788
J. Phys. Chem. A 2022, 126, 7829−7839

RESULTS AND DISCUSSION

Electronic Structure and Bonding. *Sulfur Diimide and Sulfur Dimethide Bond Lengths.* Previous studies for obtaining the ground-state geometries on heteroannulated fused ring systems having sulfur diimide bonding as well as an open-shell nature suggest that Hybrid DFT functionals having 50% of exact HF exchange fares better than the conventionally used B3LYP method.[40] In this account, from the widely used methods, we have chosen the M06-2X functional over the BH and HLYP function to estimate the geometries because the prior functional is less susceptible to symmetry breaking and minimal singlet−triplet stability issues than the latter.[11] The established bonding nature for the non-Kekule-type biradicaloids derived from tetramethylenebenzene (TMB) substructure suggests that the significant changes in geometry can be found mainly in central ring with donor substitution than the other rings.[15] Thus, selected bond lengths obtained at the M06-2X/cc-PVTZ level are provided in Table 1. In case of the sulfur diimide moiety, the increased conjugation from **TT$_0$** to **TT$_3$** has induced shortening of the S−N bond gradually. For instance, 1.601 and 1.582 Å are found for the S−N bond in **TT$_0$** and **TT$_3$**, respectively, while the other two molecules fall between. This ascertains the prominent role of sulfur for bonding within the sulfur diimide moiety of the series of molecules. Likewise, the S−C bond within the central fused thieno ring also resembles a similar change from **TT$_0$** to **TT$_3$**, that is, 1.689−1.672 Å, respectively, upholds the non-classical bonding nature of sulfur within the central fused ring in the same trend. As expected, substitution of donor groups (thienyl) at the central fused thieno ring has negligible change (0.004 Å) on sulfur diimide bond lengths. However, the central thieno ring experiences elongation in S−C bonds by 0.02 Å in all **Th-TT$_n$** molecules. This clearly suggests that the extended conjugation shortens both S−C and S−N type of bonds, while donor substitution induces significant elongation of S−C bonds in the central fused ring with negligible change in S−N bond lengths on the other end of the molecule. Hence, the characteristic long bond/singlet-biradicaloid structure within the central fused ring would be prominent along with the other non-classical bonding characters by increasing conjugation and donor substitution as well.[11,15]

Table 1. Selective Bond Lengths (in Å) and Natural Population Analysis (in e) of All the Molecules Obtained at the M06-2X/cc-PVTZ Level

			natural atomic charge			
	bond lengths[a,b]		sulfurdiimide		sulfurdimithide	
molecule	S−N	S−C	q_S	q_N	q_S	q_C
TT$_0$	1.601	1.689	1.012	−0.644	0.579	−0.462
TT$_1$	1.588	1.679	1.081	−0.645	0.616	−0.453
TT$_2$	1.584	1.676	1.119	−0.646	0.644	−0.457
TT$_3$	1.582	1.672	1.144	−0.648	0.667	−0.465
Th-TT$_0$	1.605	1.710	1.009	−0.647	0.569	−0.253
Th-TT$_1$	1.592	1.699	1.069	−0.639	0.600	−0.248
Th-TT$_2$	1.587	1.698	1.109	−0.642	0.619	−0.252
Th-TT$_3$	1.583	1.695	1.137	−0.645	0.635	−0.258

[a]Experimental bond lengths of S−N (1.77 Å), S═N (1.56 Å), S−C (1.79 Å), and S═C (1.65 Å).[66,67] [b]MP2/aug-cc-pVZ calculated bond lengths of S−C (1.80 Å) and S═C (1.60 Å).[41]

Natural Atomic Charge Analysis. The structure-bonding pattern in sulfur diimides/dimethides can be endorsed by carrying out natural population analysis. Table 1 also presents selected natural atomic charges (NACs) for the N═S═N and C═S═C bonding framework. In case of unsubstituted molecules, the NAC on sulfur in sulfur diimide (1.01e to 1.14e) is more positive than that of the sulfur dimethides (0.58e to 0.66e). In addition, the adjacent nitrogen and carbon atoms have shown NAC around −0.64e and −0.46e, respectively, suggest charge polarization is abundant toward sulfur diimide chromophore relatively. On the other hand, the substituted systems are found with insignificant changes in charge on sulfur in both the structural patterns. However, charge on carbon has been reduced to nearly half of the unsubstituted counterparts though change in charge on nitrogen is of no account. This further refers to the presence of unaltered ylidic type resonance structure within sulfur diimide, while reduced ylidic structure contribution at sulfur dimethide upon donor substitution. This is in congenial with the prediction of Fabian and Hess on a non-classical benzobisthiadazole molecule which is formally represented by tetravalent sulfur.[41]

Biradicaloid Character. Recent experimental and theoretical studies had revealed the sulfur diimide bonded heteroacenes as biradicaloids.[11,15,22,23] As it is well known that BRC alters the NLO properties, we estimate the percentage of BRC in this work. The extent of open-shell nature expressed as a percentage of BRC can be analyzed satisfactorily from the fractional occupancies of natural orbital (n_L) of orbital corresponding to LUMO of the broken symmetry wave function (eq 1). The advised DFT method for evaluation of n_L is uLC-BLYP.[42−44]

$$\%\ \mathrm{BRC} = n_L \times 100 \quad (1)$$

The calculated % BRC values are furnished in Table 2. The range for % BRC is between 0 and 100 to represent pure closed shell and pure open-shell biradical characters, respectively. The unsubstituted **TT$_0$** is found to be a pure closed-shell singlet system with no BRC, whereas DFT envisages intermediate to moderate BRC for all other molecules. As expected, the BRC increases with the expansion of π-conjugation via fused ring heteroannulation in the longitudinal axis. From **TT$_1$** to **TT$_3$**, the BRC increased from 27 to 49. On the other hand, the substitution of thienyl donor strengthens the BRC in all the molecules including **Th-TT$_0$** for which BRC is found with 39%. Similarly, substitution leads to

Table 2. uLC-BLYP/6-311g(d,p)-Derived % BRC and B3LYP/6-311G(d,p) Level-Derived Frontier Orbital Energies and HOMO−LUMO Gaps of All the Molecules Studied

molecule	% BRC	HOMO (eV)	LUMO (eV)	HLG (eV)
TT$_0$	0	−6.23	−2.82	3.41
Th-TT$_0$	39	−5.15	−3.20	1.95
TT$_1$	27	−6.37	−3.83	2.54
Th-TT$_1$	52	−5.27	−3.97	1.30
TT$_2$	40	−6.47	−4.42	2.05
Th-TT$_2$	62	−5.35	−4.48	0.87
TT$_3$	49	−6.55	−4.84	1.71
Th-TT$_3$	69	−5.42	−4.86	0.56

https://doi.org/10.1021/acs.jpca.2c04788
J. Phys. Chem. A 2022, 126, 7829−7839

more than 50% of BRC in remaining molecules, for instance, **Th-TT$_3$** attains maximum BRC among series, that is, 69%.

It is further appraised by the portrayal of OED in Figure 1.[45,46] For bare **TT$_n$**, the OED distribution is almost equally

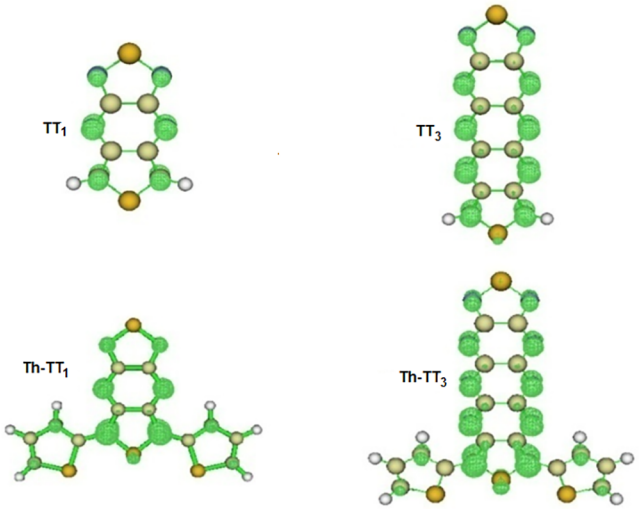

Figure 1. OED plots for **TT$_1$**, **TT$_3$**, **Th-TT$_1$**, and **Th-TT$_3$** molecules derived at the uLC-BLYP method.

distributed throughout the zig-zag edge regions. It points out that the biradicaloid is more delocalized over the longitudinal axis. Upon thienyl substitution, the amplitude of OED is slightly dominant in the substituted central thiophene ring and decreases as going toward the other end. From the same figure, one can comprehend that OED's lobes can be even seen in the 3,5-position of the thienyl group. Thus, the enhancement in BRC of the substituted derivatives hails from the OED's localization and its distribution extending toward donor sites in the longitudinal axis.

To investigate the electron delocalization pattern in these molecules, analysis of the localized orbital locator (LOL-π) plane above 2 bohr units of the molecular plane has been performed for all the molecules and given in Figure 2.[47] The regions with large LOL-π values (red and yellow) are with high electron kinetic energies and so profound delocalization is assigned, while with low values (blue) are in the boundary between localized π-orbitals. It can be inferred from the LOL-π plane maps that the participation of sulfur from the central fused ring has been minimized upon substitution of thienyl donor groups in all the cases. However, the principal delocalization path within the longitudinal axis is not affected and has contributions from all the bonds except sulfur in sulfur diimide moieties in central fused and side donor groups as well. Given all this, it seems reasonable to assume that these systems are both ylidic and biradicaloid and that the donor substitution effect increases BRC by reducing ylidic properties.

Optical Properties. *HOMO, LUMO, and HOMO–LUMO Gaps.* To explore the utility of a molecule as an optical and/or electronic active material by aiming to deduce structure activity design relationships, investigating the frontier molecular orbital (HOMO and LUMO) is inevitable. For many borderline biradicaloids, it is reported that HOMO and LUMO eigenvalues from the B3LYP method reliably reproduced the experimental electron affinities and ionization potentials, and the HLGs to a reasonable extend which corresponds to the long wavelength absorption maxima.[48] The absolute value may be slightly different but to a good approximation, the predicted trends may be ideal to understand the opto-electronic behavior of these systems. Therefore, in this study, eigenvalues of HOMO and LUMO are evaluated at the B3LYP/6-311G(d,p) level, and the obtained results are summarized in Table 2. As

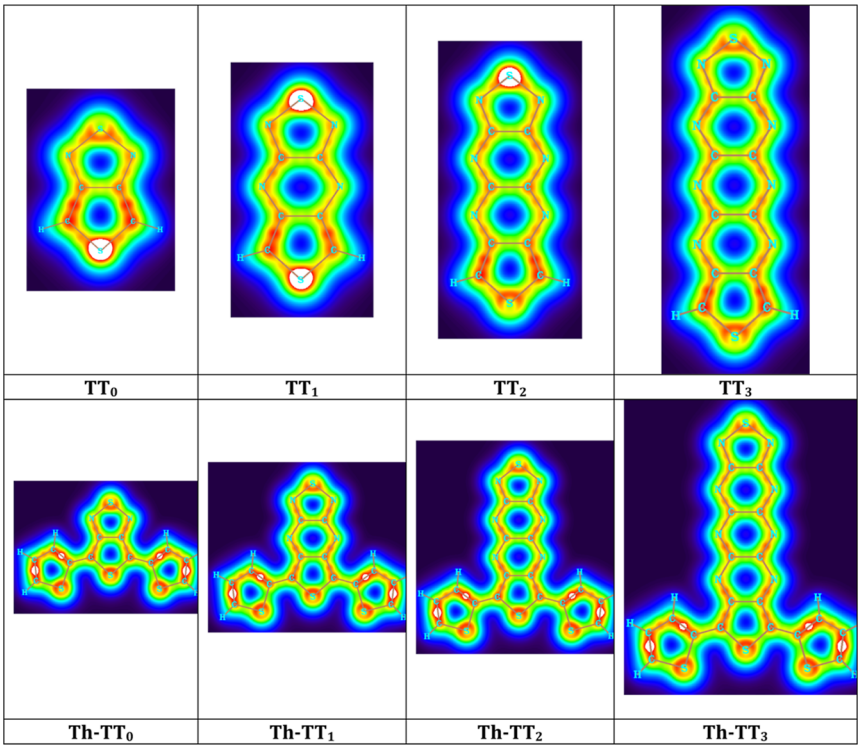

Figure 2. LOL-π plane of all the molecules obtained at the uLC-BLYP/6-311 g(d,p) level.

https://doi.org/10.1021/acs.jpca.2c04788
J. Phys. Chem. A 2022, 126, 7829–7839

Scheme 2. Schematic Representation of Oxyallyl-, TME-, and TMB-Based Biradicaloid Systems

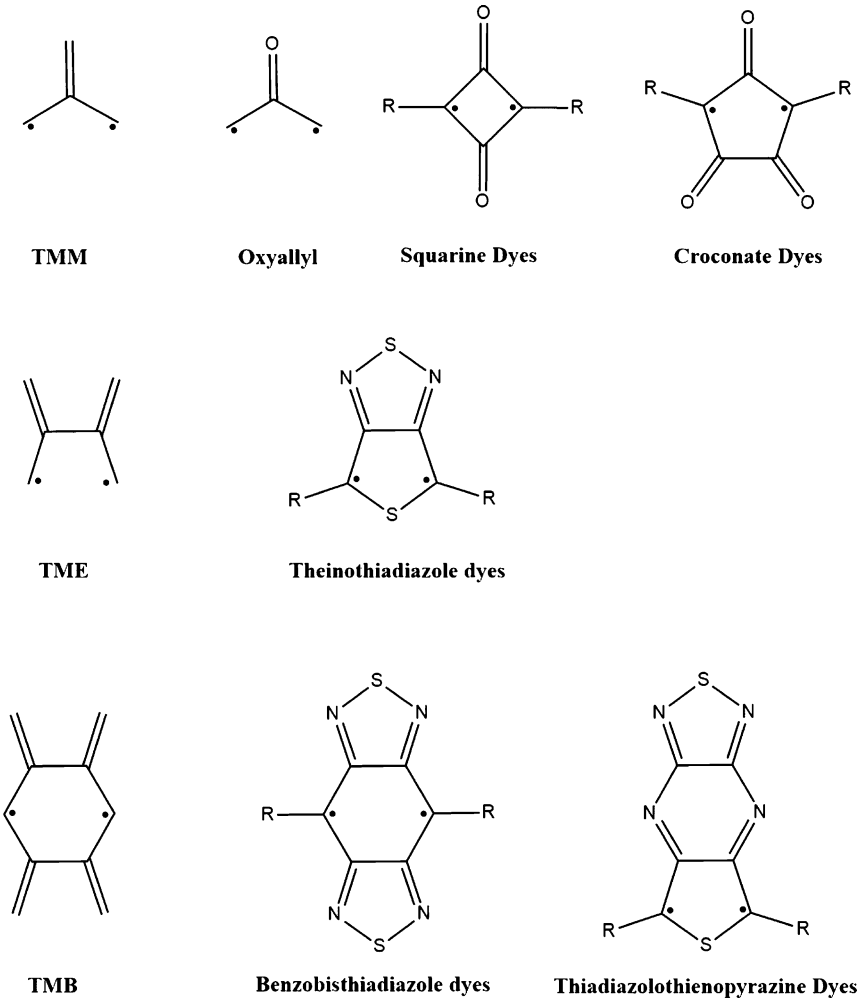

the fused ring number increases from $\mathbf{TT_0}$ to $\mathbf{TT_3}$, we could see only a mild stabilization (0.14−0.08 eV) of the HOMO level, whereas the LUMO shows a pronounced lowering in energy, that is, from $\mathbf{TT_0}$ to $\mathbf{TT_1}$ a stabilization of 1.01 eV, from $\mathbf{TT_1}$ to $\mathbf{TT_2}$ stabilizes about 0.59 eV again from $\mathbf{TT_2}$ to $\mathbf{TT_3}$ 0.42 eV. Hence, these molecules tend to show a better electron-accepting behavior as new rings are annulated and are clearly without sacrificing ionization energy. Interestingly, this feature is absolutely different from the tendency seen in linear acenes, where along with the LUMO, the HOMO is also destabilized.[49] Similarly, the extent of stabilization of HOMO and LUMO levels is found relatively small within the substituted molecules ($\mathbf{Th\text{-}TT_n}$) compared to unsubstituted counterparts. In contrast, the thiophene donor substitution largely destabilizes the HOMO to about 1.1 eV to the parent unsubstituted molecules. Furthermore, the donor group also lowers the LUMO, and this stabilization effect on LUMO is more pronounced in lower order ring systems, and as the number of fused-ring increases, the magnitude of stabilization decreases. Thus, the donor substitution destabilizes the HOMO, while the additional conjugation with fused rings in the longitudinal axis stabilizes LUMO, which helps to reduce the gap between frontier orbitals.

When compared with linear acenes and corresponding aza-acenes, the obtained HLG values are smaller for $\mathbf{TT_n}$ series, for example, considering the two-ring system, naphthalene, pyrazino[2,3-*b*]pyrazine, and $\mathbf{TT_0}$, the HLG values are 4.8, 3.9, and 3.41 eV, respectively.[49] Similarly for five-membered ring systems, the sequence is noted as pentacene (2.17 eV) > decazapentacene (2.33 eV) > $\mathbf{TT_3}$ (1.71 eV).[50] The extrapolation of the hypothesis brings that the thiophene donor substitution narrows further the HLG, which may result beyond the NIR region absorption property.

One-Photon Absorption Characteristics. In molecules with narrow HLGs, electron transitions occur in the NIR region and the NLO response is expected to be magnified.[48,51,52] In the case of non-Kekule-type biradicals with TMM substructure (oxyallyl-based dyes such as squarine and croconate, see Scheme 2) our own experience with the estimation of excitation energies using TD-DFT method has not been very encouraging.[48,53] Nevertheless, we have successfully obtained excitation energy values using DFT methods with 50% HF exchange for molecules having TMB and tetramethyleneethane substructures (benzobisthiadiazole, BBT, thienothiadiazoles, TT, see Scheme 2).[11,15,40] The success of TDDFT may be a fortuitous error−error cancellation due to considerable CT in the BBT/TT dyes (which does not exist in the case of oxyallyl dyes) cannot be completely ruled out. M06-2x functional, in comparison with BH&HLYP, is less prone to symmetry breaking.[11,15] Furthermore, it is noteworthy that Grotjahn et al. in their studies of capto-dative stabilized biradicaloids have estimated the vertical excitation energies nearly accurately with

https://doi.org/10.1021/acs.jpca.2c04788
J. Phys. Chem. A 2022, 126, 7829−7839

respect to CC2/CBS by the TD-M06 method.[54] Because of these promising results, we have begun this part of the study using the results of the TD-M06. As these molecules exhibit panchromatic absorption, we report in Table 3 the wavelengths

Table 3. One-Photon Absorption Properties of All the Molecules Obtained at the M06-2X/6-311+G(d,p) Level and CAM-B3LYP/6-311+G(d,p) Level (in Parentheses)

	excited state 1		excited state 2	
molecule	λ_{max} (nm)	f	λ_{max} (nm)	f
TT$_0$	378 [379]	0.068 [0.068]	267 [267]	0.357 [0.355]
Th-TT$_0$	640[a] [601]	0.284 [0.290]	330 [320]	0.457 [0.453]
TT$_1$	519 [511]	0.047 [0.049]	321 [322]	0.525 [0.516]
Th-TT$_1$	1022[b] [926]	0.096 [0.104]	376 [363]	0.483 [0.473]
TT$_2$	638 618	0.039 [0.042]	391 [364]	0.001 [0.718]
Th-TT$_2$	1551 [1306]	0.046 [0.058]	441 [424]	0.291 [0.264]
TT$_3$	754 [718]	0.034 [0.037]	417 [402]	0.018 [0.971]
Th-TT$_3$	2389 [1803]	0.023 [0.035]	525 [498]	0.143 [0.130]

[a]Experimental absorption maximum 624 nm.[68] [b]Experimental absorption maximum 940 nm.[69]

and oscillatory strengths of the first two dipole-allowed excited states. The increased conjugation with ring fusion shifted the absorption maximum by about 140 nm from **TT$_0$** to **TT$_1$**, as expected, while about 120 nm for both **TT$_1$** to **TT$_2$** and **TT$_2$** to **TT$_3$** cases. Hence, in **TT$_n$** derivatives, ring fusion in the longitudinal axis leads to the shift of absorption to NIR region absorption. There is a significant bathochromic shift seen for donor-substituted derivatives (**Th-TT$_n$**) as compared with their unsubstituted counterparts for both short and long wavelength region absorptions. For **Th-TT$_1$** and **Th-TT$_2$**, the predicted absorption maxima are in the NIR-II window region (1000−1750 nm). It is well known that as BRC increases, the oscillator strength decreases and the table clearly illustrates this trend.[9] It should be noted that the second absorption is more intense than the observed absorption maximum. A further comparison was made using TDDFT studies utilizing the Coulomb attenuating CAM-B3LYP functional, a range-separated hybrid DFT functional that can address CT excitations. A similar trend occurs with CAM-B3LYP and all of the wavelength maximums are blue-shifted compared to M06-2X.

TD-DFT is generally a single reference configuration approach, meaning it has inherited limitations related to addressing the open-shell nature, double excitation, and CT, making its application to elucidate excitation energies in systems with varying BRCs (especially extreme biradicaloids) always a concern. For a deeper discernment of the scope and limitations of TD-DFT, we also used post-HF methods to estimate excitation energies, such as SAC-CI, ADC(2), and the spin-flip variant of ADC(2).In the succeeding Table 4, we present the excitation energies along with the oscillator strength estimated by SAC-CI, ADC(2), and SF-ADC. The results appear to be very consistent with the TD-DFT results, although shifted to shorter wavelengths.

To explain the origin of the large red shifts within the series, we have examined the frontier molecular orbitals (FMOs) which are given in Figure 3. The long wavelength region electron excitations are predominantly HOMO to LUMO transitions. Upon inspection of LUMO pictures, the electron densities were almost similar between respective **TT$_n$** and **Th-TT$_n$** derivatives. On the contrary, in the case of HOMO,

Table 4. Absorption Maxima of Spectral Wavelength in nm Predicted in the Gas Phase by SAC-CI, ADC(2), and SF-ADC(2)[a]

molecule	SAC-CI (in nm)	ADC(2) (in nm)	SF-ADC(2)(in nm)
TT$_0$	362 (0.151)	345 (0.098)	367
Th-TT$_0$	633 (0.313)	509 (0.404)	538
TT$_1$	505 (0.112)	473 (0.070)	506
Th-TT$_1$	961 (0.156)	789 (0.138)	816
TT$_2$	607 (0.094)	580(0.060)	576
Th-TT$_2$	1170 (0.110)	1119(0.076)	1116
TT$_3$	701 (0.087)	678 (0.054)	608
Th-TT$_3$	1521 (0.076)	1518(0.049)	1240

[a]Oscillator strength in parenthesis.

regions of anti-bonding characteristics between donor and central thiophene rings were clearly visible. This leads to the narrower gap between FMOs and so the observed large shifts in absorption accordingly. Moreover, a significant decrease in orbital coefficients on the thiadiazole and pyrazine rings in HOMO from **Th-TT$_0$** to **Th-TT$_3$**. As FMOs in these derivatives are disjoint in nature, donor substitution results in an enhanced bathochromic shift.[55] In the laboratory, synthesis of these molecules might face stability issues, but recent advances have resulted in many biradicaloids with very high BRC values being synthesized and tested for optoelectronic applications.[56−58]

CT Analysis. The associated CT during one-photon absorption evaluated with TD-DFT and SAC-CI methods is presented in Table 5 based on the qualitative index proposed by Le Bahers et al.[59] As reported for biradicaloid squarylium dye derivatives, the TD-DFT and SAC-CI methodologies have shown good agreement for the CT indexes in this study too.[53] Thus, TD-DFT results at the CAM-B3LYP/6-311+G(d,p) level have been discussed in this section. The net charge transferred (Q^{ct}) is found non-significant which is below 1e, suggesting poor CT during OPA in all the molecules. However, the donor substitution induces a small CT from **Th-TT$_0$** to **Th-TT$_3$**. On the other hand, the CT length (D^{ct}) has been notably increased upon increased fused rings and donor substitution as well. The unsubstituted molecules observe D^{ct} between 1.172 and 3.113 Å, while the substituted molecules are found between 1.325 and 3.325 Å. This increased D^{ct} provides an opportunity to quantify the variation in the dipole moment (μ^{ct}). Therefore, the significance of electron donor substitution has been clearly unveiled in all cases. The unsubstituted **TT$_0$** has got 2.586 D of change in dipole, while the thiophene substitution results 3.376 D for **Th-TT$_0$**. Similarly, large dipole changes are observed in the case of **TT$_3$** and **Th-TT$_3$** as 7.849 and 12.536 D, respectively. Owing to the small Q^{ct} and large D^{ct} and μ^{ct} values, it will be required to study the overlap between centroids of charge increased and charge-depleted regions in a molecule. Interestingly, the overlap of both centroids has been found within the 0.8−0.9 range indicates that both the centroids are not well separated as expected in pure CT molecules.[53] Also the large H-index values suggest that these molecules experience poor CT but strong charge reorganization during one photon absorption.

Static Second Hyperpolarizability. Recent literature shows that calculating static hyperpolarizability with the uLC-BLYP functional with split valence basis combined with diffuse and polarization function provides results that are comparable to

https://doi.org/10.1021/acs.jpca.2c04788
J. Phys. Chem. A 2022, 126, 7829−7839

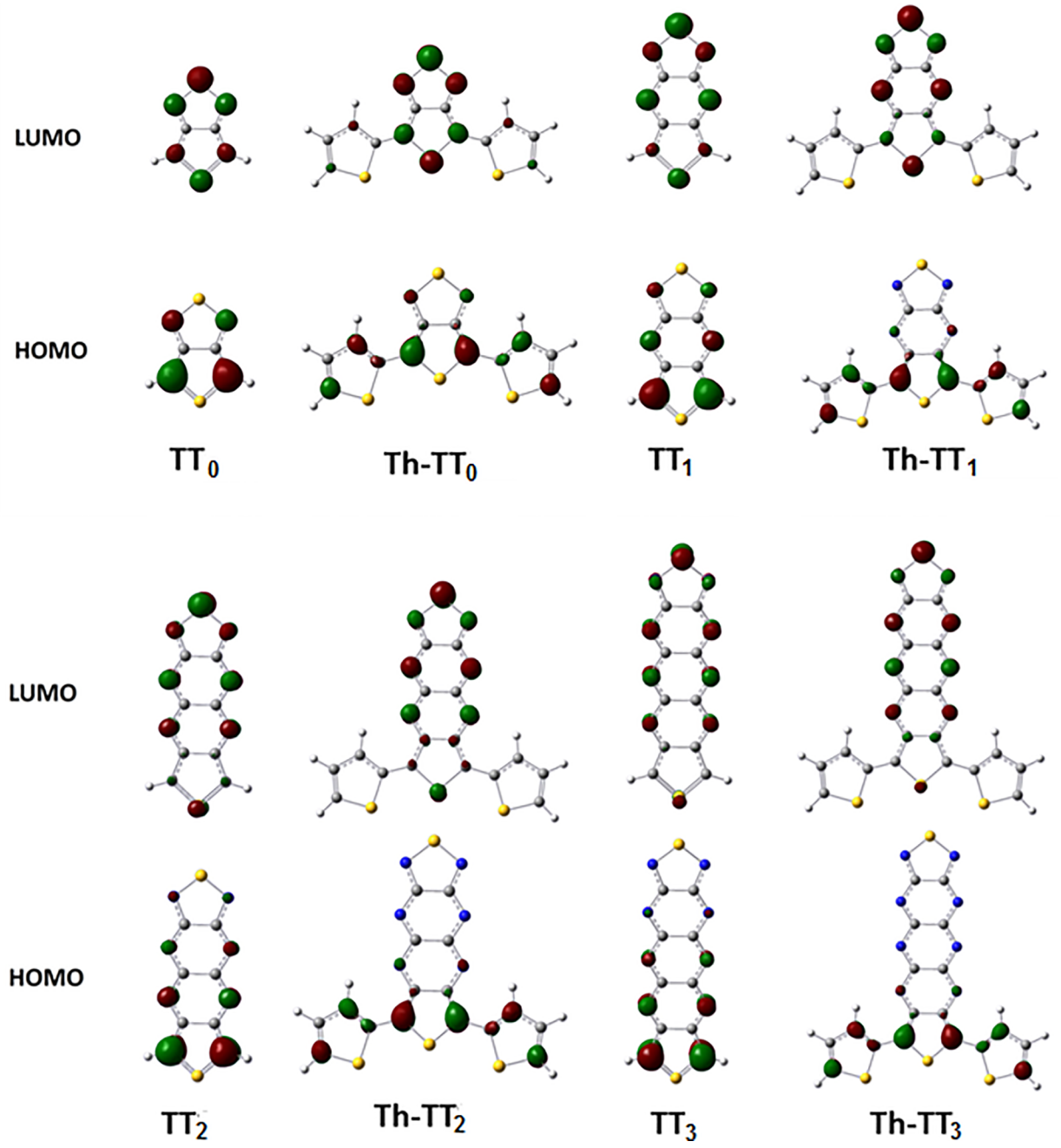

Figure 3. FMOs depicted at the M06-2X/6-311+G(d,p) level for all molecules.

Table 5. Net Charge Transferred (Q^{ct} in e), CT Length (D^{ct} in Å), Variation in Dipole Moment (μ^{CT} in debye), *H*-Index (in Å), and Overlap between Centroids of Charge Increased and Charge Depletion Regions (C^+/C^-) during One-Photon Absorption Obtained at the CAM-B3LYP/6-311++G(d,p) Level[a]

molecule Index	TT_0	Th-TT_0	TT_1	Th-TT_1	TT_2	Th-TT_2	TT_3	Th-TT_3
Q^{ct}	0.46 (0.44)	0.53 (0.55)	0.52 (0.54)	0.67 (0.73)	0.53 (0.62)	0.74 (0.82)	0.54 (0.64)	(0.86)
D^{ct}	1.172 (1.090)	1.325 (1.365)	1.733 (1.740)	2.063 (2.075)	2.336 (2.424)	2.722 (2.695)	3.113 (2.908)	3.325 (3.266)
μ^{CT}	2.586 (2.322)	3.376 (3.576)	4.284 (4.548)	6.666 (7.293)	6.110 (7.156)	9.665 (10.644)	7.849 (8.875)	12.536 (13.573)
H	2.235 (2.262)	3.294 (3.249)	2.784 (2.692)	3.599 (3.539)	3.346 (3.266)	3.993 (3.944)	3.91 (3.81)	4.415 (4.350)
C^+/C^-	0.89 (0.90)	0.84 (0.85)	0.90 (0.91)	0.82 (0.83)	0.9 (0.91)	0.81 (0.83)	0.90 (0.91)	0.80 (0.82)

[a]SAC-CI/6-31G(d,p) level results are given in parenthesis.

those achieved by the spin unrestricted CCSD method.[60,61] Therefore, the hyperpolarizability tensor components are calculated using the uLC-BLYP/6-311+G(d,p) method and presented in Table 6 for all molecules. Scheme 3 illustrates the molecule's alignment in the *XZ* plane of the Cartesian space. The origin is placed at the central thiophene ring, the donor

https://doi.org/10.1021/acs.jpca.2c04788
J. Phys. Chem. A 2022, 126, 7829−7839

Table 6. Orientationally Averaged Isotropic Second Hyperpolarizability (γ) Tensor Components of All Molecules Obtained by Using the uLC-BLYP/6-311+G(d,p) Method[a]

molecules	‖ (z)	$\gamma_{(yyyy)}$	$\gamma_{(xxxx)}$	$\gamma_{(zzzz)}$	$\gamma_{(xxzz)}$
TT$_0$	6.34	5.21	2.02	9.85	1.19
Th-TT$_0$	175.67	10.46	684.27	31.47	60.24
TT$_1$	22.88	5.11	15.90	54.76	12.06
Th-TT$_1$	221.88	10.37	562.59	229.47	137.81
TT$_2$	59.07	5.41	21.01	204.28	24.04
Th-TT$_2$	404.14	10.53	466.00	1083.57	214.71
TT$_3$	140.49	5.80	24.05	575.34	39.51
Th-TT$_3$	867.25	10.92	399.93	3270.29	312.65

[a]The magnitude is in 10^{-36} esu units.

Scheme 3. Schematic Representation of the Orientation of All Molecules in the *XZ* Plane of the Cartesian Space

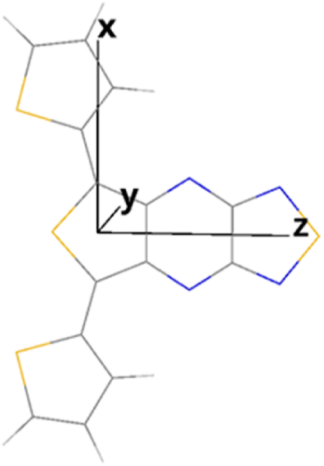

group is on the X-axis (transverse axis), while the extended conjugation reclined in the molecule through the Z-axis (longitudinal axis). The orientationally averaged isotropic second hyperpolarizability (γ) is evaluated from the following eq 2[1]

$$\gamma_{av} = \frac{1}{5}(\gamma_{xxyy} + \gamma_{xxzz} + \gamma_{yyzz} + 2\gamma_{xxxx} + 2\gamma_{yyyy} + 2\gamma_{zzzz}) \quad (2)$$

Thus, we focus on longitudinal components (Z-axis) and transverse components (X-axis), as the purpose of this study is to examine the extension of conjugation and π-donor effects. Initially, we delineate the tensor components contributing to the overall γ value for the unsubstituted series. Each of the discussed values is in the esu units of γ and needs to be multiplied by 10^{-36}. As we had aligned the molecule in the XZ-plane, the γ_{yyyy} value contribution is negligible to overall γ (with the exception of **TT$_0$**) and is in between 5 and 6. In the case of γ_{xxxx}, small increments have been found as 2.02 for **TT$_0$**, 15.90 for **TT$_1$**, 21.01 for **TT$_2$**, and 24.05 for **TT$_3$**. However, with respect to the increased conjugation in the longitudinal axis, the lowest member **TT$_0$** has a γ_{zzzz} of 9.90, while **TT$_1$** is observed with 5.5 times larger γ_{zzzz} values. Similarly, **TT$_1$** to **TT$_2$** is increased 3.7 times and then **TT$_2$** to **TT$_3$** by 2.8 times. In general, γ_{zzzz} contributes the most to overall γ value, as expected.

The effect of donor substitution has a significant role in overall γ values. The transverse component γ_{xxxx} obtains a larger value of 684 for **Th-TT$_0$**, as the donor is positioned in the X-axis. However, this value drops as the fused ring number increases. That is, the decrease in γ_{xxxx} observed in the order **Th-TT$_1$** > **Th-TT$_2$** > **Th-TT$_3$** as 562, 466, and 400, respectively. On the other hand, the longitudinal γ_{zzzz} has apparently been found to be 3−5.5 times larger than the one obtained for the unsubstituted one. The γ_{zzzz} estimates for **Th-TT$_2$** is 1084 and that of **Th-TT$_3$** is 3270 and is quite large when compared to those of other reported diradicaloid systems.[21] As can be seen in Table 6, γ_{zzzz} is a major contributor for the total γ for thienyl-substituted **Th-TT$_2$** and **Th-TT$_3$** molecules, while γ_{xxxx} sets up the overall γ for **Th-TT$_0$** and **Th-TT$_1$**. Thus, by adjusting the donor strength and conjugation, as well as by extending conjugation by ring fusion, gigantic NLO responses could be achieved. For example, comparing these longitudinal components on similar size rings such as in pentacene, the γ_{zzzz} is 13.8×10^4 au,[21] here for **TT$_3$** is 114.2×10^4 au, and upon substituting the thiophene donor, the γ_{zzzz} shoots up to 649.3×10^4 au for **Th-TT$_3$**.

Calculated Two-Photon Absorption Characteristics. The calculated two photon absorption properties such as wave-

Table 7. Two-Photon Absorption Properties and Tensor Elements Obtained at the CAM-B3LYP/6-31++G(d,p) Level

molecule	transition	ω_{0f} (eV)	2λ(nm)	S_{xx}	S_{yy}	S_{zz}	S_{xy}	S_{xz}	S_{yz}	δ (au)	σ (GM)
TT$_0$	S_0−S_{15}	6.97	356	6.5	209.2	−60.6	0	0	0	7930	282
TT$_1$	S_0−S_5	4.50	551	0	0	0	0	0	−128.1	4380	64.8
	S_0−S_7	5.10	486	0	0	0	0	0	−338.5	30600	583
TT$_2$	S_0−S_5	3.61	687	0	0	0	0	0	128.6	4410	42.1
	S_0−S_8	4.26	582	0	0	0	0	0	−512.9	70100	933
	S_0−S_{20}	6.74	368	−2.2	−9.8	1664.7	0	0	0	552000	18400
TT$_3$	S_0−S_4	3.04	816	0	0	0	0	0	130.5	4540	30.7
	S_0−S_6	3.53	703	0	0	0	−152.9	0	0	6230	56.9
	S_0−S_8	3.70	670	0	0	0	0	0	671.4	120000	1210
	S_0−S_{20}	6.20	400	1.9	−326.4	−4087.5	0	0	0	3540000	99700
Th-TT$_0$	S_0−S_2	3.89	638	0	0	0	0	0	−587.7	92100	1020
	S_0−S_3	4.07	609	0.7	24623.8	−8.7	0	0	0	121000000	1470000
	S_0−S_5	4.24	585	0.5	2266	−12.4	0	0	0	1020000	13500
Th-TT$_1$	S_0−S_3	3.42	725	0	0	0	0	0	207.5	11500	98.4
	S_0−S_4	3.44	721	−0.8	−742.2	34.2	0	0	0	107000	930

https://doi.org/10.1021/acs.jpca.2c04788
J. Phys. Chem. A 2022, 126, 7829−7839

length, transition probabilities, and absorption cross sections based on the CAM-B3LYP/6-31++G(d,p) model chemistry are presented in Table 7. The obtained TPA cross sections (σ) help to index these molecules in various applications such as in high-energy ultraviolet grade fiber optics and biological applications as well, obtained upon increasing conjugation and donor substitutions. **TT$_0$** exhibits significant TPA activity with a σ value of 282 GM at a wavelength (2λ) of 356 nm for a deeper S_0-S_{15} transition. While better TPA cross sections for **TT$_1$** than **TT$_0$** resulted with the S_0-S_7 transition, this leads to 583 GM TPA cross section exhibited for 486 nm absorption. The TPA tensors S_{yy} and S_{yz} are contributing to these TPA activities of **TT$_0$** and **TT$_1$** respectively. Going further to **TT$_2$**, we observe a better and multiple responses. Most significantly, the S_0-S_{20} transition (368 nm) possesses the strongest TPA cross section response 18 400 GM along with S_0-S_8 transition (582 nm) with 933 GM response. Between these two, the largest σ has a major contribution from S_{zz} tensor that emphasizes the charge reorganization in the longitudinal axis, while the other transition is for S_{yz}. A much stronger response can be found in **TT$_3$** with a TPA response of 1210 and 99 700 GM at 670 and 400 nm wavelengths, respectively, as well as moderate responses at 703 and 816 nm with values of 57 and 30 GM, respectively. Similar to **TT$_2$**, the largest TPA cross section among all the unsubstituted molecules has attained contribution from S_{zz} tensor which claims that the extension of conjugation in the longitudinal axis has a greater contribution in the TPA response. As others have claimed, these results affirm that extensive conjugation is essential for achieving a good TPA response.[62,63]

Upon substitution with donor, **Th-TT$_0$** shows a pronounced TPA response with 1.47×10^6 GM at 609 nm and 1020 GM at 638 nm. The other significant response falls at 585 nm with a σ of 13 500 GM. TPA does not enhance as expected further, but **Th-TT$_1$** exhibits adequate responses with σ values of 930 and 98 GM, respectively, at 721 and 725 nm. The BRC increment results in decreasing TPA activity.[64,65] Currently, we are reluctant to discuss TPA for **Th-TT$_2$** and **Th-TT$_3$** because our maximum TPA excitation energy for these systems is negative, which might be a result of their large BRC, which would require more correlated ab initio methods.

CONCLUSIONS

The presence of π-donor thienyl substitution in the transverse axis and extension of conjugation in the longitudinal axis by increasing pyrazine rings incorporates a quadrupolar nature in nonclassical oligo-pyrazinothienthiadiazole derivatives. Accordingly, two sets of molecules are considered in this study, one for increasing conjugation in longitudinal axes (**TT$_n$**, $n = 0-3$) and the second one for having additional π-donor thienyl substitution at the central thienyl group in the transverse axis (**Th-TT$_n$**, $n = 0-3$). The resulting changes in geometry, NAC, and frontier orbital energies have been analyzed by using DFT methodologies by which the asymmetric nature of geometry and charge distribution is unveiled. The inspection of frontier orbitals in all the derivatives has shown that the π-donor destabilizes the HOMO, while additional conjugation stabilizes LUMO levels. Thus, the narrowing of the gap between frontier orbitals not only introduces but also enhances the BRC accordingly. The odd electron densities (OEDs) and associated π-ELF have been plotted to investigate the electron distribution in these molecules. The OED plots reveal that large electron densities are found near the central thienyl ring, while zig-zag mannered charge clouds in the longitudinal axis. Similarly, π-ELF plots proclaim the poor contribution from sulfur atoms in the central thiophene ring and side π-donor thienyl substitutions as well. This indicates the unaltered ylidic character in sulfur diimide chromophore, while reduced ylidic character in the substituted thiophene ring along with the presence of long-bond/singlet BRC in sulfur dimethide part in both the series. Also, these effects lead to the panchromatic one-photon absorption by all the molecules. To address the CT associated with one photon absorption, Le Baher's indices have been considered and found that the net CT is very less contradictory to D^{ct} which is increased in both the series of molecules. This has been interpreted by the overlap of charge gain and charge loss regions (C^+/C^-) and H-index by which the charge reorganization is concluded instead of the CT nature during electron transition.

The non-linear optical activities of all molecules have been evaluated by studying second-order hyperpolarizability (γ) and TPA cross-sectional values associated with tensor values in all the molecules. From **TT$_0$-TT$_3$**, the tensors in the longitudinal axis are found to be the major contributors to the overall γ response. In the case of **Th-TT$_n$** derivatives, tensors in the transverse axis have larger contributions for **Th-TT$_0$** and **Th-TT$_1$**, while longitudinal tensors play a major role in the large γ response in the rest two molecules. Similarly, TPA characteristics are also found with the same behavior in tensor contributions to the increased TPA cross sections in **TT$_n$** series. However, the π-donor thienyl substitution seems to be disadvantageous in **Th-TT$_n$** series as TPA cross sections are dampening from $n = 0-1$ though shift in transverse to the longitudinal axis is ascertained.

AUTHOR INFORMATION

Corresponding Authors

Siddlingeshwar B − *Department of Physics, M.S. Ramaiah Institute of Technology, (Autonomous Institute Affiliated to VTU), Bengaluru 560054, India;* orcid.org/0000-0001-6681-6203; Email: sidduphysics@gmail.com

Krishna Chaitanya Gunturu − *School of Chemical Sciences, S.R.T.M. University, Nanded 431606 Maharashtra, India;* orcid.org/0000-0001-6634-8905; Email: kc.gunturu@srtmun.ac.in

Anna Kaczmarek-Kędziera − *Faculty of Chemistry, Nicolaus Copernicus University in Toruń, 87-100 Toruń, Poland;* orcid.org/0000-0002-4931-8701; Email: teoadk@chem.umk.pl

Authors

Anup Thomas − *Centre for Computational Research in Clean Energy Technologies, Sree Chitra Thirunal College of Engineering, Trivandrum 695018, India*

Mahesh G. Wakhradkar − *School of Chemical Sciences, S.R.T.M. University, Nanded 431606 Maharashtra, India*

Joel Abraham − *Centre for Computational Research in Clean Energy Technologies, Sree Chitra Thirunal College of Engineering, Trivandrum 695018, India*

Complete contact information is available at: https://pubs.acs.org/10.1021/acs.jpca.2c04788

Notes

The authors declare no competing financial interest.

https://doi.org/10.1021/acs.jpca.2c04788
J. Phys. Chem. A 2022, 126, 7829−7839

■ ACKNOWLEDGMENTS

K.C.G. thanks CSIR, New Delhi, India for the financial assistance throughout this research project 01(3079)/21/EMR-II.

■ REFERENCES

(1) Bredas, J. L.; Adant, C.; Tackx, P.; Persoons, A.; Pierce, B. M. Third-Order Nonlinear Optical Response in Organic Materials: Theoretical and Experimental Aspects. *Chem. Rev.* **1994**, *94*, 243−278.

(2) Williams, D. J. Organic Polymeric and Non-Polymeric Materials with Large Optical Nonlinearities. *Angew. Chem.Angew. Chem., Int. Ed. Engl. Int. Ed. Engl.* **1984**, *23*, 690−703.

(3) Prasad, P. N.; Williams, D. J.*Introduction to Nonlinear Optical Effects in Molecules and Polymers*; John Wiley & Sons: Nashville, TN, 1991.

(4) Pascal, S.; David, S.; Andraud, C.; Maury, O. Near-Infrared Dyes for Two-Photon Absorption in the Short-Wavelength Infrared: Strategies towards Optical Power Limiting. *Chem. Soc. Rev.* **2021**, *50*, 6613−6658.

(5) Lou, A. J.-T.; Marks, T. J. A Twist on Nonlinear Optics: Understanding the Unique Response of π-Twisted Chromophores. *Acc. Chem. Res.* **2019**, *52*, 1428−1438.

(6) Hales, J. M.; Matichak, J.; Barlow, S.; Ohira, S.; Yesudas, K.; Brédas, J.-L.; Perry, J. W.; Marder, S. R. Design of Polymethine Dyes with Large Third-Order Optical Nonlinearities and Loss Figures of Merit. *Science* **2010**, *327*, 1485−1488.

(7) Yesudas, K.; Bhanuprakash, K. Origin of Near-Infrared Absorption and Large Second Hyperpolarizability in OxyallylDiradicaloids: A Three-State Model Approach. *J. Phys. Chem. A* **2007**, *111*, 1943−1952.

(8) Nakano, M.; Fujita, H.; Takahata, M.; Yamaguchi, K. Theoretical Study on Second Hyperpolarizabilities of Phenylacetylene Dendrimer: Toward an Understanding of Structure-Property Relation in NLO Responses of Fractal Antenna Dendrimers. *J. Am. Chem. Soc.* **2002**, *124*, 9648−9655.

(9) Fabian, J.; Zahradník, R. The Search for Highly Colored Organic Compounds. *Angew. Chem.Angew. Chem., Int. Ed. Engl. Int. Ed. Engl.* **1989**, *28*, 677−694.

(10) Verbiest, T.; Clays, K.; Samyn, C.; Wolff, J.; Reinhoudt, D.; Persoons, A. Investigations of the Hyperpolarizability in Organic Molecules from Dipolar to Octopolar Systems. *J. Am. Chem. Soc.* **1994**, *116*, 9320−9323.

(11) Thomas, A.; Ji, C.; Siddlingeshwar, B.; Manohar, P. U.; Ying, F.; Wu, W. Revealing the Biradicaloid Nature Inherited in the Derivatives of Thieno[3,4-c][1,2,5]Thiadiazole: A Computational Study. *Phys. Chem. Chem. Phys.* **2021**, *23*, 1050−1061.

(12) Dressler, J. J.; Haley, M. M. Learning How to Fine-tune Diradical Properties by Structure Refinement. *J. Phys. Org. Chem.* **2020**, *33*, No. e4114.

(13) Nakano, M. Electronic Structure of Open-Shell Singlet Molecules: Diradical Character Viewpoint. *Top. Curr. Chem. (J)* **2017**, *375*, 47.

(14) Puyad, A. L.; Prabhakar, C.; Yesudas, K.; Bhanuprakash, K.; Jayathirtha Rao, V. High-Level Computational Studies of Rhodizonate Derivatives: Molecules Absorbing in near Infrared Region Due to Larger C−C−C Angle of the Oxyallyl Ring. *Theochem* **2009**, *904*, 1−6.

(15) Thomas, A.; Krishna Chaitanya, G.; Bhanuprakash, B.; Krishna Prasad, M. M. Substituents Destabilize the Molecule by Increasing Biradicaloid Character and Stabilize by Intramolecular Charge Transfer in the Derivatives of Benzobis(Thiadiazole) and Thiadiazolothienopyrazine: A Computational Study. *Chemphyschem* **2011**, *12*, 3458−3466.

(16) Kishi, R.; Murata, Y.; Saito, M.; Morita, K.; Abe, M.; Nakano, M. Theoretical Study on Diradical Characters and Nonlinear Optical Properties of 1,3-Diradical Compounds. *J. Phys. Chem. A* **2014**, *118*, 10837−10848.

(17) Fukuda, K.; Matsushita, N.; Minamida, Y.; Matsui, H.; Nagami, T.; Takamuku, S.; Kitagawa, Y.; Nakano, M. Impact of Diradical/Ionic Character on Third-Order Nonlinear Optical Property in Asymmetric Phenalenyl Dimers. *ChemistrySelect* **2017**, *2*, 2084−2087.

(18) Ishida, M.; Shin, J.-Y.; Lim, J. M.; Lee, B. S.; Yoon, M.-C.; Koide, T.; Sessler, J. L.; Osuka, A.; Kim, D. Neutral Radical and Singlet Biradical Forms of Meso-Free, -Keto, and −DiketoHexaphyrins(1.1.1.1.1.1): Effects on Aromaticity and Photophysical Properties. *J. Am. Chem. Soc.* **2011**, *133*, 15533−15544.

(19) Motomura, S.; Nakano, M.; Fukui, H.; Yoneda, K.; Kubo, T.; Carion, R.; Champagne, B. Size Dependences of the Diradical Character and the Second Hyperpolarizabilities in Dicyclopenta-Fused Acenes: Relationships with Their Aromaticity/Antiaromaticity. *Phys. Chem. Chem. Phys.* **2011**, *13*, 20575−20583.

(20) Nakano, M.; Champagne, B. Nonlinear Optical Properties in Open-Shell Molecular Systems: NLO Properties in Open-Shell Molecular Systems. *Wiley Interdiscip. Rev. Comput. Mol. Sci.* **2016**, *6*, 198−210.

(21) Nakano, M.; Fukuda, K.; Champagne, B. Third-Order Nonlinear Optical Properties of Asymmetric Non-Alternant Open-Shell Condensed-Ring Hydrocarbons: Effects of Diradical Character, Asymmetricity, and Exchange Interaction. *J. Phys. Chem. C Nanomater. Interfaces* **2016**, *120*, 1193−1207.

(22) Yuen, J. D.; Wang, M.; Fan, J.; Sheberla, D.; Kemei, M.; Banerji, N.; Scarongella, M.; Valouch, S.; Pho, T.; Kumar, R.; Chesnut, E. C.; Bendikov, M.; Wudl, F. Importance of Unpaired Electrons in Organic Electronics. *J. Polym. Sci. A Polym. Chem.* **2015**, *53*, 287−293.

(23) Chen, Z.; Li, W.; Sabuj, M. A.; Li, Y.; Zhu, W.; Zeng, M.; Sarap, C. S.; Huda, M. M.; Qiao, X.; Peng, X.; Ma, D.; Ma, Y.; Rai, N.; Huang, F. Evolution of the Electronic Structure in Open-Shell Donor-Acceptor Organic Semiconductors. *Nat. Commun.* **2021**, *12*, 5889.

(24) Qian, G.; Wang, Z. Y. Near-Infrared Organic Compounds and Emerging Applications. *Chem.—Asian J.* **2010**, *5*, 1006−1029.

(25) Lee, W.-H.; Cho, M.; Jeon, S.-J.; Cho, B. R. Two-Photon Absorption and Second Hyperpolarizability of the Linear Quadrupolar Molecule. *J. Phys. Chem. A* **2000**, *104*, 11033−11040.

(26) Hirao, K.; Nakatsuji, H. Cluster Expansion of the Wavefunction. *Chem. Phys. Lett.* **1981**, *79*, 292−298.

(27) Dreuw, A.; Wormit, M. The Algebraic Diagrammatic Construction Scheme for the Polarization Propagator for the Calculation of Excited States. *Wiley Interdiscip. Rev.: Comput. Mol. Sci.* **2015**, *5*, 82−95.

(28) Lefrancois, D.; Tuna, D.; Martínez, T. J.; Dreuw, A. The Spin-Flip Variant of the Algebraic-Diagrammatic Construction Yields the Correct Topology of S_1/S_0 Conical Intersections. *J. Chem. Theory Comput.* **2017**, *13*, 4436−4441.

(29) Lu, T.; Chen, F. M. A Multifunctional WavefunctionAnalyzer. *J. Comput. Chem.* **2012**, *33*, 580−592.

(30) Paterson, M. J.; Christiansen, O.; Pawłowski, F.; Jørgensen, P.; Hättig, C.; Helgaker, T.; Sałek, P. Benchmarking Two-Photon Absorption with CC3 Quadratic Response Theory, and Comparison with Density-Functional Response Theory. *J. Chem. Phys.* **2006**, *124*, 054322.

(31) Lescos, L.; Sitkiewicz, S. P.; Beaujean, P.; Blanchard-Desce, M.; Champagne, B.; Matito, E.; Castet, F. Performance of DFT Functionals for Calculating the Second-Order Nonlinear Optical Properties of Dipolar Merocyanines. *Phys. Chem. Chem. Phys.* **2020**, *22*, 16579−16594.

(32) Day, P. N.; Nguyen, K. A.; Pachter, R. Calculation of Two-Photon Absorption Spectra of Donor-Pi-Acceptor Compounds in Solution Using Quadratic Response Time-Dependent Density Functional Theory. *J. Chem. Phys.* **2006**, *125*, 094103.

(33) Beerepoot, M. T. P.; Friese, D. H.; List, N. H.; Kongsted, J.; Ruud, K. Benchmarking two-photon absorption cross sections: performance of CC2 and CAM-B3LYP. *Phys. Chem. Chem. Phys.* **2015**, *17*, 19306.

(34) Beerepoot, M. T. P.; Alam, Md M.; Bednarska, J.; Bartkowiak, W.; Ruud, K.; Zaleśny, R. Benchmarking the Performance of

https://doi.org/10.1021/acs.jpca.2c04788
J. Phys. Chem. A 2022, 126, 7829−7839

Exchange-Correlation Functionals for Predicting Two-Photon Absorption Strengths. *J. Chem. Theory Comput.* **2018**, *14*, 3677−3685.
(35) Chołuj, M.; Alam, Md. M.; Beerepoot, M. T. P.; Sitkiewicz, S. P.; Matito, E.; Ruud, K.; Zaleśny, R. Choosing Bad versus Worse: Predictions of Two-Photon-Absorption Strengths Based on Popular Density Functional Approximations. *J. Chem. Theory Comput.* **2022**, *18*, 1046−1060.
(36) Frisch, M. J.; Trucks, G. W.; Schlegel, H. B.; Scuseria, G. E.; Robb, M. A.; Cheeseman, J. R.; Scalmani, G.; Barone, V.; Petersson, G. A.; Nakatsuji, H.; Li, X.; et al.*Gaussian 16*, Revision C.01, 2016.
(37) Aidas, K.; Angeli, C.; Bak, K. L.; Bakken, V.; Bast, R.; Boman, L.; Christiansen, O.; Cimiraglia, R.; Coriani, S.; Dahle, P.; et al. The Dalton Quantum Chemistry Program System: The Dalton Program. *Wiley Interdiscip. Rev.: Comput. Mol. Sci.* **2014**, *4*, 269−284.
(38) Dalton/LSDalton program. http://daltonprogram.org (accessed June 27, 2022).
(39) Epifanovsky, E.; Gilbert, A. T. B.; Feng, X.; Lee, J.; Mao, Y.; Mardirossian, N.; Pokhilko, P.; White, A. F.; Coons, M. P.; Dempwolff, A. L.; et al. Software for the Frontiers of Quantum Chemistry: An Overview of Developments in the Q-Chem 5 Package. *J. Chem. Phys.* **2021**, *155*, 084801.
(40) Thomas, A.; Bhanuprakash, K.; Prasad, K. M. M. K. Near Infrared Absorbing Benzobis(Thiadiazole) Derivatives: Computational Studies Point to Biradical Nature of the Ground States: NEAR INFRARED ABSORBING BENZOBIS(THIADIAZOLE) DERIVATIVES. *J. Phys. Org. Chem.* **2011**, *24*, 821−832.
(41) Fabian, J.; Hess, B. A. $\lambda 4\sigma 2$-Sulfur Heterocycles. An Ab Initio and Density Functional Study. *J. Org. Chem.* **1997**, *62*, 1766−1774.
(42) Nakano, M.; Kubo, T.; Kamada, K.; Ohta, K.; Kishi, R.; Ohta, S.; Nakagawa, N.; Takahashi, H.; Furukawa, S.-I.; Morita, Y.; Nakasuji, K.; Yamaguchi, K. Second Hyperpolarizabilities of Polycyclic Aromatic Hydrocarbons Involving Phenalenyl Radical Units. *Chem. Phys. Lett.* **2006**, *418*, 142−147.
(43) Yamaguchi, K. The Electronic Structures of Biradicals in the Unrestricted Hartree-Fock Approximation. *Chem. Phys. Lett.* **1975**, *33*, 330−335.
(44) Yamanaka, S.; Okumura, M.; Nakano, M.; Yamaguchi, K. EHF Theory of Chemical Reactions Part 4. UNO CASSCF, UNO CASPT2 and R(U)HF Coupled-Cluster (CC) Wavefunctions. *J. Mol. Struct.* **1994**, *310*, 205−218.
(45) Takatsuka, K.; Fueno, T.; Yamaguchi, K. Distribution of Odd Electrons in Ground-State Molecules. *Theoret. Chim. Acta* **1978**, *48*, 175−183.
(46) Head-Gordon, M. Characterizing Unpaired Electrons from the One-Particle Density Matrix. *Chem. Phys. Lett.* **2003**, *372*, 508−511.
(47) Schmider, H. L.; Becke, A. D. Two Functions of the Density Matrix and Their Relation to the Chemical Bond. *J. Chem. Phys.* **2002**, *116*, 3184−3193.
(48) Thomas, A.; Srinivas, K.; Prabhakar, C.; Bhanuprakash, K.; Rao, V. J. Estimation of the First Excitation Energy in DiradicaloidCroconate Dyes Having Absorption in the near Infra Red (NIR): A DFT and SF-TDDFT Study. *Chem. Phys. Lett.* **2008**, *454*, 36−41.
(49) Winkler, M.; Houk, K. N. Nitrogen-Rich Oligoacenes: Candidates for n-Channel Organic Semiconductors. *J. Am. Chem. Soc.* **2007**, *129*, 1805−1815.
(50) Thomas, A.; Chitumalla, R. K.; Puyad, A. L.; Mohan, K. V.; Jang, J. Computational Studies of Hole/Electron Transport in Positional Isomers of Linear Oligo-Thienoacenes: Evaluation of Internal Reorganization Energies Using Density Functional Theory. *Comput. Theor. Chem.* **2016**, *1089*, 59−67.
(51) Kamada, K.; Ueda, M.; Nagao, H.; Tawa, K.; Sugino, T.; Shmizu, Y.; Ohta, K. Molecular Design for Organic Nonlinear Optics: Polarizability and Hyperpolarizabilities of Furan Homologues Investigated by Ab Initio Molecular Orbital Method. *J. Phys. Chem. A* **2000**, *104*, 4723−4734.
(52) Nakano, M.; Kishi, R.; Ohta, S.; Takebe, A.; Takahashi, H.; Furukawa, S.-I.; Kubo, T.; Morita, Y.; Nakasuji, K.; Yamaguchi, K.; Kamada, K.; Ohta, K.; Champagne, B.; Botek, E. Origin of the Enhancement of the Second Hyperpolarizability of Singlet Diradical Systems with Intermediate Diradical Character. *J. Chem. Phys.* **2006**, *125*, 074113.
(53) Krishna Chaitanya, G.; Puyad, L. A.; Bhanuprakash, K. Charge Transfer or Biradicaloid Character: Assessing TD-DFT and SAC-CI for Squarylium Dye Derivatives. *RSC Adv.* **2015**, *5*, 18813−18821.
(54) Grotjahn, R.; Maier, T. M.; Michl, J.; Kaupp, M. Development of a TDDFT-Based Protocol with Local Hybrid Functionals for the Screening of Potential Singlet Fission Chromophores. *J. Chem. Theory Comput.* **2017**, *13*, 4984−4996.
(55) Fabian, J. TDDFT-Calculations of Vis/NIR Absorbing Compounds. *Dyes Pigm.* **2010**, *84*, 36−53.
(56) Barker, J. E.; Dressler, J. J.; Cárdenas Valdivia, A.; Kishi, R.; Strand, E. T.; Zakharov, L. N.; MacMillan, S. N.; Gómez-García, C. J.; Nakano, M.; Casado, J.; Haley, M. M. Molecule Isomerism Modulates the Diradical Properties of Stable Singlet Diradicaloids. *J. Am. Chem. Soc.* **2020**, *142*, 1548−1555.
(57) Dressler, J. J.; Teraoka, M.; Espejo, G. L.; Kishi, R.; Takamuku, S.; Gómez-García, C. J.; Zakharov, L. N.; Nakano, M.; Casado, J.; Haley, M. M. Thiophene and Its Sulfur Inhibit IndenoindenodibenzothiopheneDiradicals from Low-Energy Lying Thermal Triplets. *Nat. Chem.* **2018**, *10*, 1134−1140.
(58) Dressler, J. J.; Barker, J. E.; Karas, L. J.; Hashimoto, H. E.; Kishi, R.; Zakharov, L. N.; MacMillan, S. N.; Gomez-Garcia, C. J.; Nakano, M.; Wu, J. I.; Haley, M. M. Late-Stage Modification of Electronic Properties of Antiaromatic and DiradicaloidIndeno[1,2-b]Fluorene Analogues via Sulfur Oxidation. *J. Org. Chem.* **2020**, *85*, 10846−10857.
(59) Le Bahers, T.; Adamo, C.; Ciofini, I. A Qualitative Index of Spatial Extent in Charge-Transfer Excitations. *J. Chem. Theory Comput.* **2011**, *7*, 2498−2506.
(60) Bonness, S.; Botek, E.; Champagne, B. Long-Range Corrected Density Functional Theory Study on Static Second Hyperpolarizabilities of Singlet Diradical Systems. *J. Chem. Phys.* **2010**, *132*, 094107.
(61) de Wergifosse, M.; Champagne, B. Electron Correlation Effects on the First Hyperpolarizability of Push-Pull π-Conjugated Systems. *J. Chem. Phys.* **2011**, *134*, 074113.
(62) Pawlicki, M.; Collins, H. A.; Denning, R. G.; Anderson, H. L. Two-Photon Absorption and the Design of Two-Photon Dyes. *Angew. Chem. Int. Ed Engl.* **2009**, *48*, 3244−3266.
(63) Belfield, K. D.; Yao, S.; Bondar, M. V.Two-Photon Absorbing Photonic Materials: From Fundamentals to Applications. In *Photoresponsive Polymers I*; Springer Berlin Heidelberg: Berlin, Heidelberg, 2008; pp 97−156.
(64) Nakano, M.; Yoneda, K.; Kishi, R.; Takahashi, H.; Kubo, T.; Kamada, K.; Ohta, K.; Champagne, B.; Botek, E. One- and Two-Photon Absorptions in Open-Shell Singlet Systems. *AIP Conf. Proc.* **2012**, *1504*, 136.
(65) Botek, M.; Champagne, K.; Kishi, R.; Takahashi, H.; Kubo, T.; Kamada, K.; Ohta, K.; Botek, E.; Champagne, B. Remarkable Two-Photon Absorption in Open-Shell Singlet Systems. *J. Chem. Phys.* **2009**, *131*, 114316.
(66) Parker, T. C.; Patel, D. G.; Moudgil, K.; Barlow, S.; Risko, C.; Brédas, J.-L.; Reynolds, J. R.; Marder, S. R. Heteroannulated Acceptors Based on Benzothiadiazole. *Mater. Horiz.* **2015**, *2*, 22−36.
(67) Fabian, J.; Hess, B. A., Jr. Sulfur-Containing Mesoionic Compounds: Theoretical Study on Structure and Properties. *Int. J. Quantum Chem.* **2002**, *90*, 1055−1063.
(68) Canola, S.; Mardegan, L.; Bergamini, G.; Villa, M.; Acocella, A.; Zangoli, M.; Ravotto, L.; Vinogradov, S. A.; Di Maria, F.; Ceroni, P.; Negri, F. One- and Two-Photon Absorption Properties of Quadrupolar Thiophene-Based Dyes with Acceptors of Varying Strengths. *Photochem. Photobiol. Sci.* **2019**, *18*, 2180−2190.
(69) Tanaka, S.; Yamashita, Y. A Novel Monomer Candidate for Intrinsically Conductive Organic Polymers Based on Nonclassical Thiophene. *Synth. Met.* **1997**, *84*, 229−230.

https://doi.org/10.1021/acs.jpca.2c04788
J. Phys. Chem. A 2022, 126, 7829−7839